INSTITUTE OF PHYSICS PUBLISHING NANOTECHNOLOGY
Nanotechnology **16** (2005) 2346–2353 doi:10.1088/0957-4484/16/10/059

The bactericidal effect of silver nanoparticles

Jose Ruben Morones[1], Jose Luis Elechiguerra[1], Alejandra Camacho[2], Katherine Holt[3], Juan B Kouri[4], Jose Tapia Ramírez[5] and Miguel Jose Yacaman[1,2]

[1] Department of Chemical Engineering, University of Texas at Austin, Austin, TX 78712, USA
[2] Texas Materials Institute, University of Texas at Austin, Austin, TX 78712, USA
[3] Department of Chemistry and Biochemistry, University of Texas at Austin, Austin, TX 78712, USA
[4] Departamento de Patología Experimental, Centro de Investigaciones y de Estudios Avanzados del Instituto Politécnico Nacional (CINVESTAV-IPN), Avenida IPN 2508, Colonia San Pedro de Zacatenco, CP 07360, México DF, Mexico
[5] Departamento de Genética y Biología Molecular, Centro de Investigaciones y de Estudios Avanzados del Instituto Politécnico Nacional (CINVESTAV-IPN), Avenida IPN 2508, Colonia San Pedro de Zacatenco, CP 07360, México DF, Mexico

Received 21 June 2005, in final form 13 July 2005
Published 26 August 2005
Online at stacks.iop.org/Nano/16/2346

Abstract
Nanotechnology is expected to open new avenues to fight and prevent disease using atomic scale tailoring of materials. Among the most promising nanomaterials with antibacterial properties are metallic nanoparticles, which exhibit increased chemical activity due to their large surface to volume ratios and crystallographic surface structure. The study of bactericidal nanomaterials is particularly timely considering the recent increase of new resistant strains of bacteria to the most potent antibiotics. This has promoted research in the well known activity of silver ions and silver-based compounds, including silver nanoparticles. The present work studies the effect of silver nanoparticles in the range of 1–100 nm on Gram-negative bacteria using high angle annular dark field (HAADF) scanning transmission electron microscopy (STEM). Our results indicate that the bactericidal properties of the nanoparticles are size dependent, since the only nanoparticles that present a direct interaction with the bacteria preferentially have a diameter of ∼1–10 nm.

(Some figures in this article are in colour only in the electronic version)

1. Introduction

The development of new resistant strains of bacteria to current antibiotics [1] has become a serious problem in public health; therefore, there is a strong incentive to develop new bactericides [2]. This makes current research in bactericidal nanomaterials particularly timely.

Bacteria have different membrane structures which allow a general classification of them as Gram-negative or Gram-positive. The structural differences lie in the organization of a key component of the membrane, peptidoglycan. Gram-negative bacteria exhibit only a thin peptidoglycan layer (∼2–3 nm) between the cytoplasmic membrane and the outer membrane [3]; in contrast, Gram-positive bacteria lack the outer membrane but have a peptidoglycan layer of about 30 nm thick [4].

Silver has long been known to exhibit a strong toxicity to a wide range of micro-organisms [5]; for this reason silver-based compounds have been used extensively in many bactericidal applications [6, 7]. It is worth mentioning some examples such as inorganic composites with a slow silver release rate that are currently used as preservatives in a variety of products; another current application includes new compounds composed of silica gel microspheres, which contain a silver

thiosulfate complex, that are mixed into plastics for long-lasting antibacterial protection [7]. Silver compounds have also been used in the medical field to treat burns and a variety of infections [8].

The bactericidal effect of silver ions on micro-organisms is very well known; however, the bactericidal mechanism is only partially understood. It has been proposed that ionic silver strongly interacts with thiol groups of vital enzymes and inactivates them [9, 10]. Experimental evidence suggests that DNA loses its replication ability once the bacteria have been treated with silver ions [8]. Other studies have shown evidence of structural changes in the cell membrane as well as the formation of small electron-dense granules formed by silver and sulfur [8, 11]. Silver ions have been demonstrated to be useful and effective in bactericidal applications, but due to the unique properties of nanoparticles nanotechnology presents a reasonable alternative for development of new bactericides.

Metal particles in the nanometre size range exhibit physical properties that are different from both the ion and the bulk material. This makes them exhibit remarkable properties such as increased catalytic activity due to morphologies with highly active facets [12–17]. In this work we tested silver nanoparticles in four types of Gram-negative bacteria: *E. coli*, *V. cholera*, *P. aeruginosa* and *S. typhus*. We applied several electron microscopy techniques to study the mechanism by which silver nanoparticles interact with these bacteria. We used high angle annular dark field (HAADF) scanning transmission electron microscopy (STEM), and developed a novel sample preparation that avoids the use of heavy metal based compounds such as OsO_4. High resolutions and more accurate x-ray microanalysis were obtained.

2. Experimental procedure

The silver nanoparticles used in this work were synthesized by Nanotechnologies, Inc. The final product is a powder of silver nanoparticles inside a carbon matrix, which prevents coalescence during synthesis. The silver nanoparticle powder is suspended in water in order to perform the interaction of the silver nanoparticles with the bacteria; for homogenization of the suspension a Cole-Parmer 8891 ultrasonic cleaner (UC) is used. The particles in solution are characterized by placing a drop of the homogeneous suspension in a transmission electron microscope (TEM) copper grid with a lacy carbon film and then using a JEOL 2010-F TEM at an accelerating voltage of 200 kV.

As a first step, several concentrations of silver nanoparticles (0, 25, 50, 75 and 100 μg ml^{-1}) were tested against each type of bacteria. Agar plates from a solution of agar, Luria–Bertani (LB) medium broth and the different concentrations of silver nanoparticles were prepared, followed by the plating of a 10 μl sample of a log phase culture with an optical density of 0.5 at 595 nm and 37 °C.

The interaction with silver nanoparticles was analysed by growing each of the bacteria to a log phase at an optical density at 595 nm of approximately 0.5 at 37 °C in LB culture medium. Then, silver nanoparticles were added to the solution, making a homogeneous suspension of 100 μg ml^{-1} and leaving the bacteria to grow for 30 min. The cells are collected by centrifugation (3000 rpm, 5 min, 4 °C), washed and then re-suspended with a PBS buffer solution. A 10 μl sample drop was deposited on TEM copper grids with a lacy carbon film and the grid was then exposed to glutaraldehyde vapours for 3 h in order to fix the bacterial sample. The bacteria were analysed in a JEOL 2010-F TEM equipped with an Oxford EDS unit at an accelerating voltage of 200 kV in scanning mode using the HAADF detector, in order to determine the distribution and location of the silver nanoparticles, as well as the morphology of the bacteria after the treatment with silver nanoparticles.

In order to have a more profound understanding of the bactericidal mechanism of the silver nanoparticles we used a different sample preparation technique. *E. coli* samples, previously exposed to silver nanoparticles, following the same procedure of interaction mentioned above, were then fixed by exposure to a 2.5% glutaraldehyde solution in PBS for 30 min, followed by a dehydration of the cells using a series of 50, 60, 80, 90 and 100% ethanol/PBS solutions and exposing the sample for ten minutes to each solution in increasing order of ethanol concentration. The cells were finally embedded into Spurr resin and left to polymerize in an oven at 60 °C for 24 h. The polymerized samples were sectioned in slices of thickness of ∼60 nm. We were then able to analyse the interior of the bacteria in the TEM in STEM mode. The same procedure but with 100 μg ml^{-1} of ionic silver, from a 1 mM solution of $AgNO_3$, was performed to compare effects of silver in ionic and nanoparticle form.

TEM analysis using sample staining was also carried out. The sample preparation followed the same procedure as the cross-sectioned sample slices but before the dehydration process the cells were tinted with a 2% OsO_4 /cacodylate buffer for 1 h. These samples were analysed in a JEOL 2000 at an accelerating voltage of 100 kV.

The electrochemical behaviour of silver nanoparticles in water solution was also analysed. Stripping voltammetry of silver nanoparticles, in dissolution in an electrolyte solution, was carried out using a 25 μm diameter platinum ultra-microelectrode. To detect silver (I) electrochemically at low concentrations, it is necessary to electro-deposit silver onto the electrode surface in a pre-concentration step by holding the potential of the electrode at −0.3 V versus Ag/AgCl for 60 s [18]. This procedure reduces Ag^+ to Ag^0, which plates onto the electrode surface. When the potential is swept positively from −0.3 to +0.35 V, the deposited silver is oxidized to Ag^+ and stripped from the electrode, giving a characteristic stripping peak with a height proportional to the concentration of Ag^+ in the solution.

3. Results and discussions

TEM analysis of the silver nanoparticles used in this work showed that the particles tend to be agglomerated inside the carbon matrix (inset figure 1(a)). However, due to the porosity of the carbon and possibly the energy provided by the UC, a significant number of nanoparticles that have been released from the carbon matrix are observed (figure 1(a)). Analysis of the released particles showed a mean size of 16 nm with a standard deviation of 8 nm. Since these nanoparticles were released from the carbon matrix, they can be considered as free

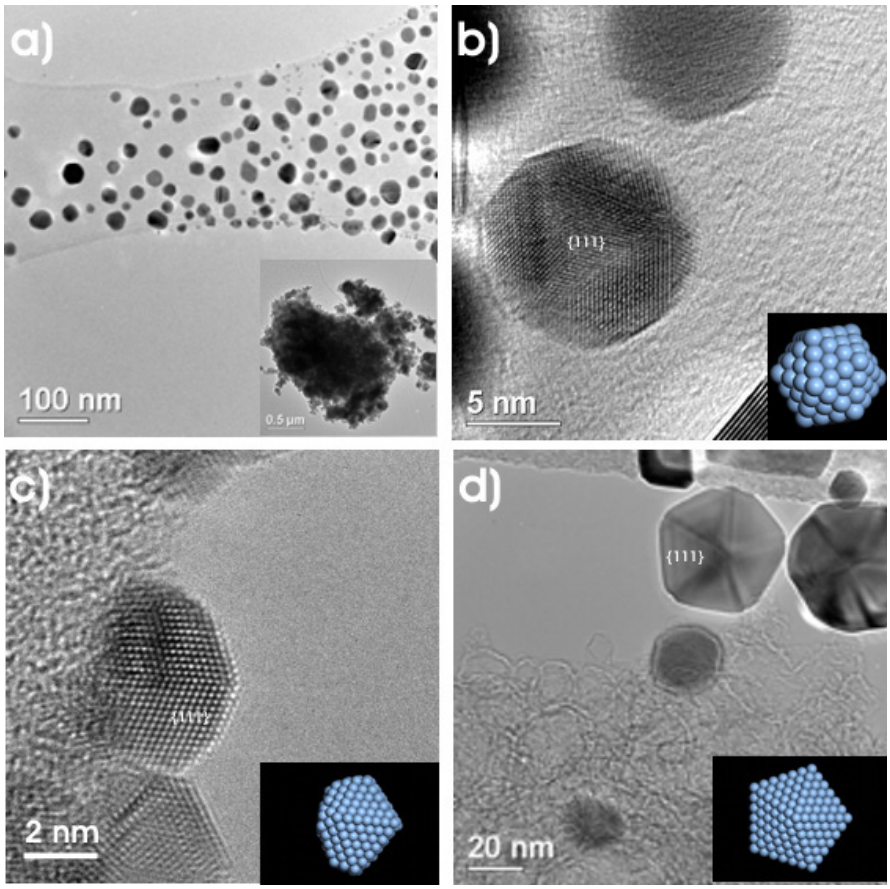

Figure 1. Silver nanoparticles. (a) TEM image of the silver nanoparticles that have been released from the carbon matrix; the inset illustrates the agglomerated particles in the carbon matrix. (b)–(d) Most common morphologies of the particles used. The {111} facets are labelled and their respective models are shown as insets: (b) icosahedral particle, (c) twinned particle and (d) decahedral particle seen in the [100] direction.

surface particles, which will enhance their reactivity compared with the nanoparticles that remained inside the carbon matrix.

An interesting phenomenon occurs when the TEM electron beam is condensed in the nanoparticle agglomerates; sufficient energy is provided for the nanoparticles remaining in the carbon matrix to be released, and the general size distribution of the nanoparticles is obtained: a mean size of 21 nm and a standard deviation of 18 nm. High resolution transmission electron microscopy (HRTEM) demonstrates that ∼95% of the particles have cuboctahedral and multiple-twinned icosahedral and decahedral morphologies (figures 1(b)–(d)). All of these morphologies present mainly {111} surfaces. Different work done on the reactivity of silver has demonstrated that the reactivity is favoured by high atom density facets such as {111} [19, 20]. Thus, a high reactivity of the nanoparticles used in this study in comparison to other particles that contain less {111} facet percentages is expected.

Each of the bacteria was tested with different concentrations of silver nanoparticles in order to observe the effect on bacterial growth. The results demonstrated that the concentration of silver nanoparticles that prevents bacteria growth is different for each type, the *P. aeruginosa* and *V. cholera* being more resistant than *E. coli* and *S. typhus*. However, at concentrations above 75 μg ml^{-1} there was no significant growth for any of the bacteria (figure 2(a)).

The results shown in figures 2(b) and (c) suggest that HAADF is useful in determining the presence of even very small (∼1 nm) silver nanoparticles on the bacteria without the use of heavy-metal staining. This is mainly due to the fact that HAADF images are formed by electrons that have been scattered at high angles due to mainly Rutherford-like scattering. As a result, the image contrast is related to the differences of atomic number (Z) in the sample with intensity varying as $\sim Z^2$ [21, 22]. The difference in the atomic number of the metal nanoparticles (silver) and the organic material (bacteria) generates an ample contrast in the images.

STEM analysis of the polymerized slices showed the interior of the bacteria and demonstrated that the nanoparticles are not only found on the surface of the cell membrane but also inside the bacteria (figures 3(a)–(c)). This was confirmed by an elemental mapping analysis using the x-ray energy dispersive spectrometer (EDS) in the TEM (figure 3(a)). The nanoparticles were found distributed all throughout the cell; they were attached to the membrane and were also able to penetrate the bacteria.

Only individual particles were observed to attach to the surface of the membrane and no clear interaction of the bacteria membrane with the agglomerates of particles in the carbon matrix was seen. This provides sufficient evidence to state that only the particles that were able to leave the carbon matrix

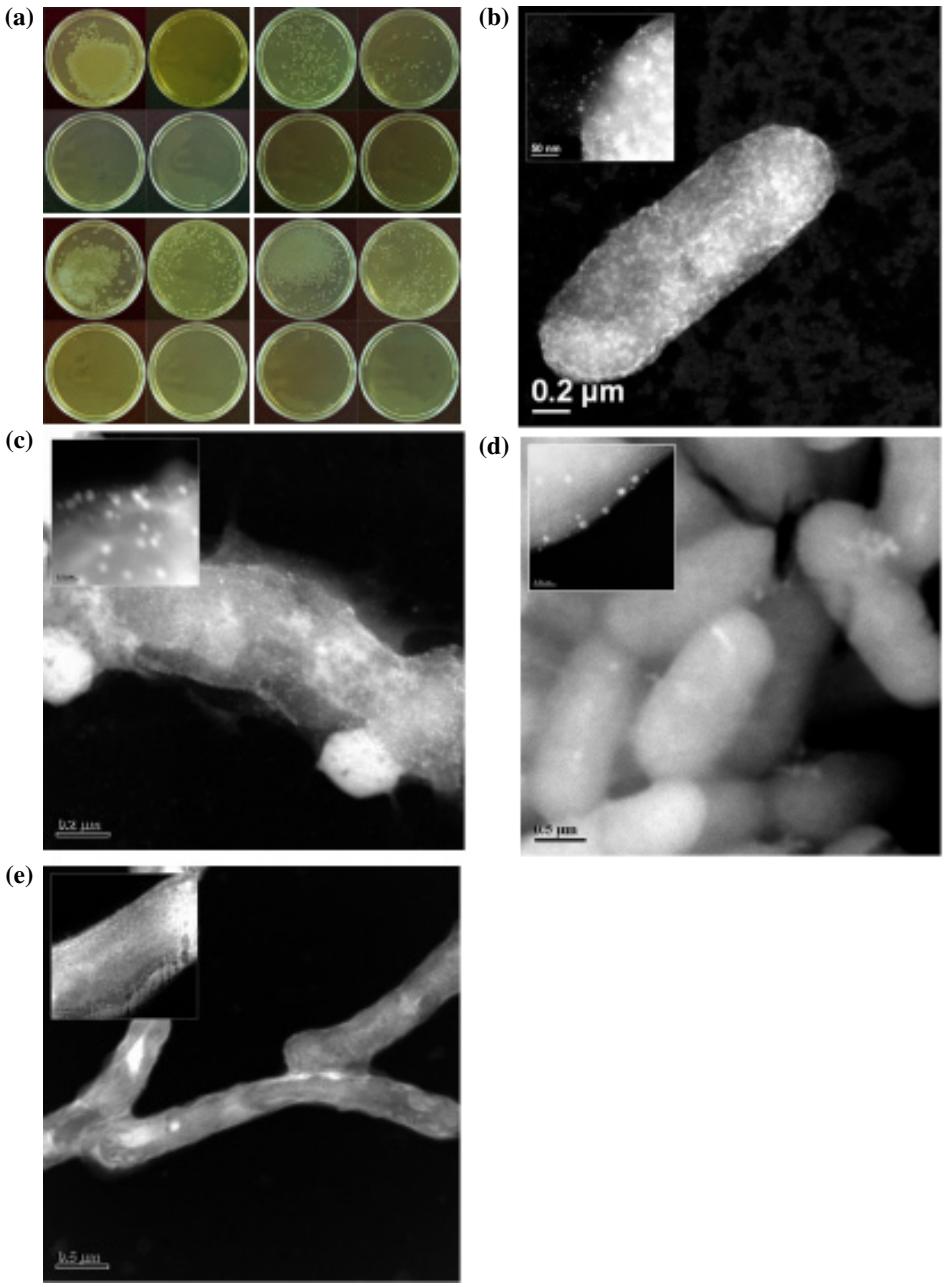

Figure 2. (a) Bacteria grown on agar plates at different concentrations of silver nanoparticles. Upper left, *E. coli*; upper right, *S. typhus*; bottom left, *P. aeruginosa*, and bottom right, *V. cholerae*. 0 μg ml^{-1} (upper left), 25 μg ml^{-1} (upper right), 50 μg ml^{-1} (bottom left) and 75 μg ml^{-1} (bottom right). HAADF STEM images that show the interaction of the bacteria with the silver nanoparticles: (b) *E. coli*, (c) *S. typhus*, (d) *P. aeruginosa* and (e) *V. cholerae*. The insets correspond to higher magnification images.

interact with the bacteria. In addition, the nanoparticles found inside the cells are of similar sizes to the ones interacting with the membrane (figures 3(b)–(c)); this implies that only the particles that interact with the membrane are able to get inside the bacteria.

Higher magnification images illustrate that the nanoparticles found on the surface of the membrane are very likely to be faceted (figure 4(a)). Figure 4(b) is a surface plot using the intensity profiles of the region enclosed in figure 4(a). Figure 4(b) was constructed with Image J, software by the National Institute of Health. As explained before, the contrast of the STEM images is mainly proportional to Z2. The intensity of the image is related to the number of electrons scattered, while the probability that an electron interacts with the nucleus of an atom is directly proportional to the thickness of the sample [23]. Since we are analysing the silver particles on the surface of the membrane, the atomic weight can be considered constant; so the intensities will be exclusively due to the thickness of the particle. The thickness profile of the particle exhibits faceting and a planar face. This suggests the interaction of a decahedral particle, which only has {111} facets.

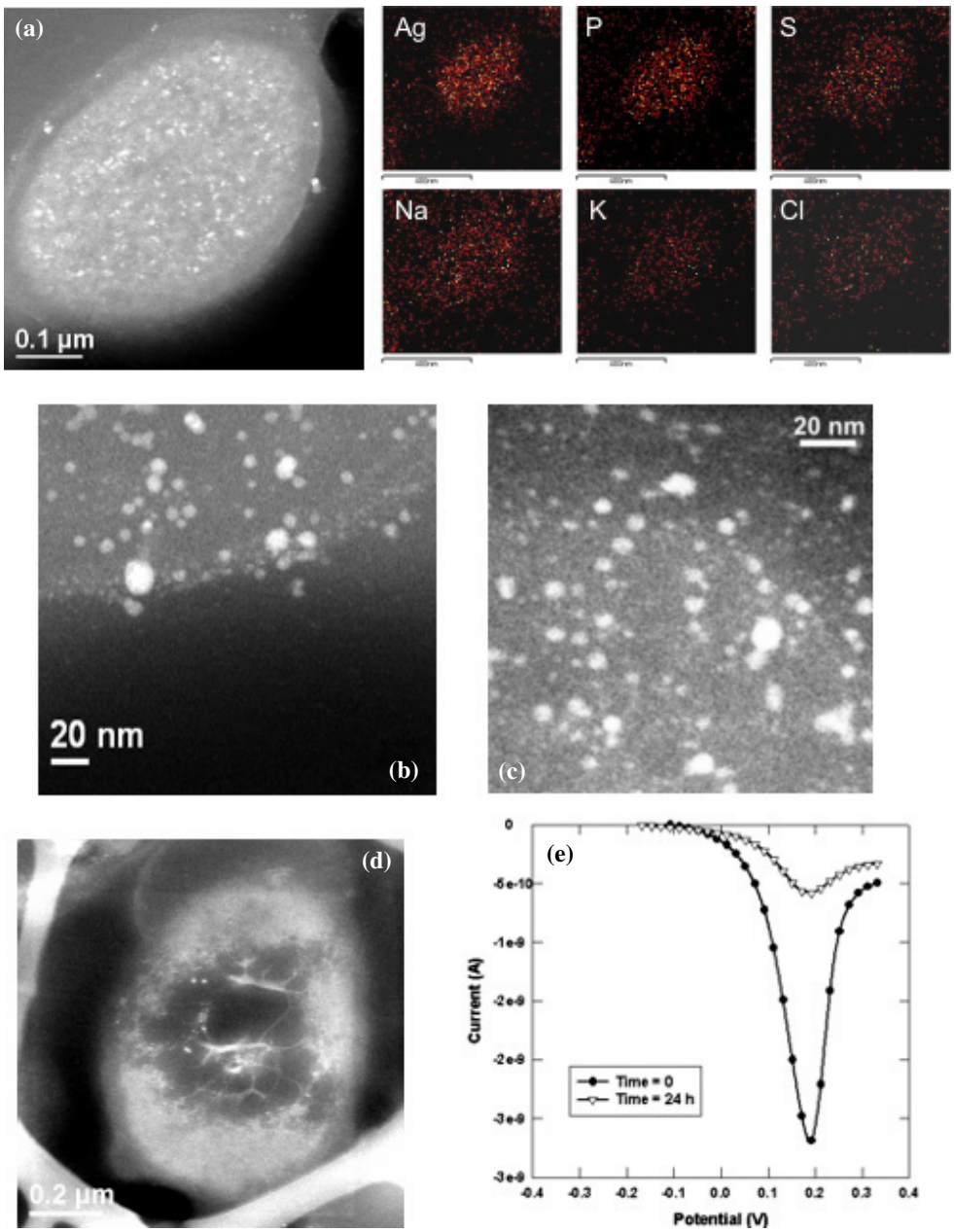

Figure 3. (a) Left: a considerable presence of silver nanoparticles is found in the membrane and the inside of an *E. coli* sample. Right: EDS elemental mapping. It can be observed that silver is well distributed through the sample. (b) Amplification of the *E. coli* membrane, where the presence of silver nanoparticles is clearly observed. (c) A close-up of the interior of an *E. coli* sample treated with silver nanoparticles. Again, the presence of silver nanoparticles is noted. (d) Image of an *E. coli* sample treated with silver nitrate, where a clear difference versus the nanoparticle treated sample is observed. As previously reported (3), a low molecular weight centre region is observed. (e) Stripping voltammetry results obtained for freshly dissolved silver nanoparticles in 0.2 M $NaNO_3$ and the curve for the same solution measured 24 h later.

The size distribution of the nanoparticles interacting with each type of bacteria was obtained from the HAADF images. The mean size of these silver nanoparticles was ∼5 nm with a standard deviation of 2 nm. The size distribution of particles found interacting directly with *E. coli* is shown in figure 4(d). This distribution corresponds to the lower end of the size distribution for the released silver nanoparticles (mean size of 16 nm with a standard deviation of 8 nm). It is clear that the bactericidal effect of the silver nanoparticles is size dependent.

The effective silver concentration was estimated using the general size distribution described in the manuscript (mean size of 21 nm and a standard deviation of 18 nm) and three hypotheses: (1) all the nanoparticles smaller than ∼10 nm interact with the bacteria; (2) the nanoparticles are spherical and (3) the amount of carbon in the sample can be discarded. If we consider the weight of the nanoparticles using the general size distribution, the results indicate that the weight percentage of nanoparticles between 1 and 10 nm corresponds

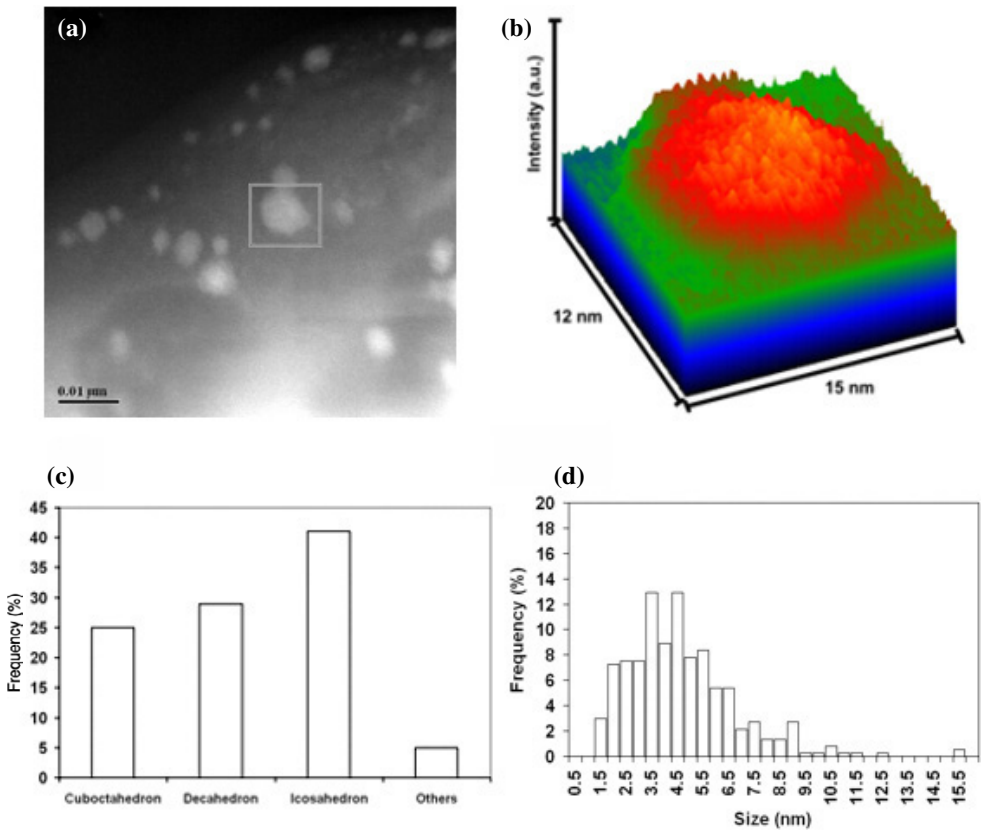

Figure 4. (a) Z-contrast image of *S. typhus*, where we are able to see silver nanoparticles faceted in the membrane of the bacteria. (b) Intensity profile of the localized region in (a). (c) Morphology distribution of the nanoparticles used that have diameters of ∼1–10 nm. (d) Size distribution, from several HAADF images, of the nanoparticles that are seen to have interaction with *E. coli*.

to 0.093% of the sample. Even when this value seems to be small, it corresponds to a large number of nanoparticles per millilitre considering the silver nanoparticle concentration of 75 μg ml^{-1} found to be effective for all the bacteria. A mean diameter of ∼5 nm and a silver density of 1.05×10^{-14} μg nm^{-3} were used to approximate the number of particles between 1 and 10 nm ml^{-1}, $\sim 9.8 \times 10^{10}$. Therefore, since the bacterial culture used in our work had an OD of 0.5, which corresponds to $\sim 5 \times 10^7$ colony forming units (cfu) per ml of solution, the ratio between the number of silver nanoparticles and cells will be ∼2000.

A statistical study of the morphologies of the particles between 1 and 10 nm showed that ∼98% of the particles are octahedral and multiple-twinned icosahedral and decahedral in shape. Several reports demonstrate the high reactivity of high density silver {111} facets [12, 15–17, 24, 25]. These previous studies and our analysis of the thickness plot of the nanoparticles found in the surface of the bacteria corroborates the faceting of the particles as well as the direct interaction of the {111} facets.

Metal particles of small sizes (∼5 nm) present electronic effects, which are defined as changes in the local electronic structure of the surface due to size. These effects are reported to enhance the reactivity of the nanoparticle surfaces [26]. In addition, it is reasonable to propose that the binding strength of the particles to the bacteria will depend on the surface area of interaction. A higher percentage of the surface will have a direct interaction in smaller particles than bigger particles; these two reasons mentioned before might explain the presence of only particles of ∼1–10 nm.

The results obtained for the bacteria using HAADF were compared using TEM and staining with OsO_4. The morphologies of the bacteria as well as the effects of the particles with the bacteria in TEM mode (figure 5) were very like those of STEM (figures 3(a)–(c). The silver nanoparticles are observed to be located in the membrane of the bacteria as well as in the interior of it. This corroborates the usefulness of the technique employed in this paper, TEM analysis using HAADF in STEM mode.

The mechanism by which the nanoparticles are able to penetrate the bacteria is not totally understood, but a previous report by Salopek suggests that in the case of *E. coli* treated with silver nanoparticles the changes created in the membrane morphology may produce a significant increase in its permeability and affect proper transport through the plasma membrane [2]. In our case, this mechanism could explain the considerable numbers of silver nanoparticles found inside the bacteria (figure 3(c)).

The observation of silver nanoparticles attached to the cell membrane (figures 2(b)–(e)) and inside the bacteria (figures 3(a)–(c) is fundamental in the understanding of the bactericidal mechanism. As established by the theory of hard and soft acids and bases, silver will tend to have a higher affinity to react with phosphorus and sulfur compounds [19, 20, 27].

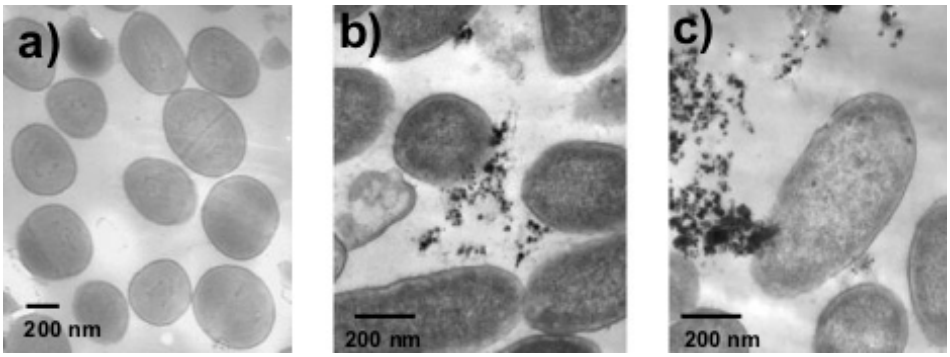

Figure 5. TEM images of a *P. aeruginosa* sample at different magnifications are shown. (a) Control sample, i.e. no silver nanoparticles were used; (b) and (c) samples that were previously treated with silver nanoparticles. Silver nanoparticles can be appreciated inside the bacteria and noticeable damage in the cell membrane can be seen when compared with the control sample.

The membrane of the bacteria is well known to contain many sulfur-containing proteins [28]; these might be preferential sites for the silver nanoparticles. On the other hand, nanoparticles found inside will also tend to react with other sulfur-containing proteins in the interior of the cell, as well as with phosphorus-containing compounds such as DNA [8]. To conclude, the changes in morphology presented in the membrane of the bacteria, as well as the possible damage caused by the nanoparticles reacting with the DNA, will affect the bacteria in processes such as the respiratory chain, and cell division, finally causing the death of the cell [28].

The possibility of a contribution of silver ions that may be present in the nanoparticle solution to the bactericidal effect of the nanoparticles was tested. To do this, we analysed the electrochemical behaviour of the nanoparticles using stripping voltammetry. As can be seen in figure 3(e), a stripping peak is obtained for silver nanoparticles freshly dissolved in 0.2 M $NaNO_3$, along with a peak obtained for the same solution 24 h later. Upon comparison with peak heights obtained from solutions of known concentration, it can be seen that Ag^+ is immediately released at a concentration of $\sim$1 μM. The solution was retested after 24 h, where it was found that the concentration of Ag^+ had decreased considerably ($\sim$0.2 μM). The data suggest that rapid Ag^+ release occurs when the nanoparticles are first dissolved, but only at levels of $<$5 μM. No further dissolution occurs and the free Ag^+ concentration decreases, possibly due to reduction processes to form Ag^0-containing clusters or re-association with the original nanoparticles. This analysis corroborated the presence of micro-molar concentrations of silver ions, which will have a contribution to the biocidal action of the silver nanoparticles.

In order to more clearly illustrate the difference in the effect of silver nanoparticles and pure ionic silver, a control experiment was performed using silver nitrate ($AgNO_3$) as biocide. The results can be seen in figures 3(a) and (d); the overall effect of the silver nanoparticles is different from the effect of only silver ions. The silver ions produce the formation of a low molecular weight region in the centre of the bacteria. This low density region formation is a mechanism of defence, by which the bacteria conglomerates its DNA to protect it from toxic compounds when the bacteria senses a disturbance of the membrane [8]. However, we did not find evidence of the formation of a low density region, rich in agglomerated DNA, as reported by Feng and collaborators, when nanoparticles are used; the bacteria instead present a large number of small silver nanoparticles inside the bacteria.

Electrostatic forces might be an additional cause for the interaction of the nanoparticles with the bacteria. It has been reported in the literature that, at biological pH values, the overall surface of the bacteria is negatively charged due to the dissociation of an excess number of carboxylic and other groups in the membrane [29]. On the other hand the nanoparticles are embedded in a carbon matrix (insulator), where there is definitely friction of the nanoparticles due to their movement inside the matrix; this will perhaps create a charge on the surface. For these reasons it is possible to expect an electrostatic attraction of the nanoparticles and the bacteria. This kind of interaction presents an interesting study for our future work.

4. Conclusions

Silver nanoparticles used in this work exhibit a broad size distribution and morphologies with highly reactive facets, {111}. We have identified that silver nanoparticles act primarily in three ways against Gram-negative bacteria: (1) nanoparticles mainly in the range of 1–10 nm attach to the surface of the cell membrane and drastically disturb its proper function, like permeability and respiration; (2) they are able to penetrate inside the bacteria and cause further damage by possibly interacting with sulfur- and phosphorus-containing compounds such as DNA; (3) nanoparticles release silver ions, which will have an additional contribution to the bactericidal effect of the silver nanoparticles such as the one reported by Feng. [8].

We have applied HAADF-STEM in this study and found it to be very useful in the study of bactericidal effects of silver particles, and it can be extended to other related research.

Acknowledgments

This work was conducted under support of Air Products and Chemicals, Inc. The authors want to thank Nanotechnologies, Inc. for providing the silver nanoparticles for this study. We would also like to thank Drs George Georgiou and Allen J Bard for letting us use their laboratories for the biological

and electrochemical testing of the silver nanoparticles. We would also like to thank Maria Magdalena Miranda from the Departamento de Patología Experimental and Carlos Cruz Cruz from the Departamento de Genética Unidad de Microscopia Electrónica of the CINVESTAV-Mexico. J R Morones, J L Elechiguerra and A Camacho-Bragado acknowledge the support received from CONACYT-México.

References

[1] Kyriacou S V, Brownlow W J and Xu X-H N 2004 *Biochemistry* **43** 140–7
[2] Sondi I and Salopek-Sondi B 2004 *J. Colloid Interface Sci.* **275** 177–82
[3] Murray R G E, Steed P and Elson H E 1965 *Can. J. Microbiol.* **11** 547
[4] Shockman G D and Barret J F 1983 *Annu. Rev. Microbiol.* **37** 501
[5] Liau S Y *et al* 1997 *Lett. Appl. Microbiol.* **25** 279–83
[6] Nomiya K *et al* 2004 *J. Inorg. Biochem.* **98** 46–60
[7] Gupta A and Silver S 1998 *Nat. Biotechnol.* **16** 888
[8] Feng Q L *et al* 2000 *J. Biomed. Mater. Res.* **52** 662–8
[9] Matsumura Y *et al* 2003 *Appl. Environ. Microbiol.* **69** 4278–81
[10] Gupta A, Maynes M and Silver S 1998 *Appl. Environ. Microbiol.* **64** 5042–5
[11] Nover L, Scharf K D and Neumann D 1983 *Mol. Cell. Biol.* **3** 1648–55
[12] Yacaman M J *et al* 2001 *J. Vac. Sci. Technol.* B **19** 1091–103
[13] Somorjai G 2004 *Nature* **430** 730
[14] Haruta M 1997 *Catal. Today* **36** 115–23
[15] Doraiswamy N and Marks L D 1996 *Surf. Sci.* **348** 67–9
[16] Iijima S and Ichihashi T 1986 *Phys. Rev. Lett.* **56** 616–9
[17] Ajayan P M and Marks L D 1988 *Phys. Rev. Lett.* **60** 585–7
[18] Jeffrey C A, Storr W M and Harrington D A 2004 *J. Electroanal. Chem.* **569** 61–70
[19] Hatchett D W and Henry S 1996 *J. Phys. Chem.* **100** 9854–9
[20] Vitanov T and Popov A 1983 *J. Electroanal. Chem.* **159** 437–41
[21] Howie A, Marks L D and Pennycook S J 1982 *Ultramicroscopy* **8** 163–74
[22] James E M and Browning N D 1999 *Ultramicroscopy* **78** 125–39
[23] Liu C P, Preston A R, Boothroyd C B and Humphreys C J 1999 *J. Microsc.* **194** 171–82
[24] Smith D J *et al* 1986 *Science* **233** 872–5
[25] Liu H B *et al* 2001 *Surf. Sci.* **491** 88–98
[26] Raimondi F, Scherer G G, Kotz R and Wokaun A 2005 *Angew. Chem. Int. Edn Engl.* **44** 2190–209
[27] Ahrland S, Chatt J and Davies N R 1958 *Q. Rev. Chem. Soc.* **12** 265–76
[28] Alcamo I E 1997 *Fundamentals of Microbiology* 5th edn (Reading, MA: Addison Wesley Longman Inc.)
[29] Stoimenov P, Klinger R, Marchin G L and Klabunde K J 2002 *Langmuir* **18** 6679–86